Nanoscale

Accepted Manuscript

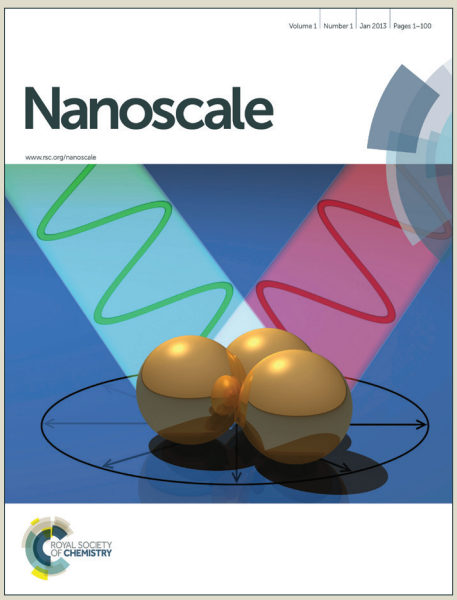

ROYAL SOCIETY OF CHEMISTRY

www.rsc.org/nanoscale

Nanoscale

RSCPublishing

ARTICLE

Adsorption and adhesion of common serum proteins to nanotextured gallium nitride

Cite this: DOI: 10.1039/xoxxoooooox

Lauren E. Bain[a], Marc P. Hoffmann[b], Isaac Bryan[b], Ramón Collazo[b], and Albena Ivanisevic[a,b]

Received ooth January 2012,
Accepted ooth January 2012

DOI: 10.1039/xoxxoooooox

www.rsc.org/

As the broader effort towards device and material miniaturization progresses in all fields, it becomes increasingly important to understand the implications of working with functional structures that approach the size scale of molecules, particularly when considering biological systems. It is well known that thin films and nanostructures feature different optical, electrical, and mechanical properties from their bulk composites; however, interactions taking place at the interface between nanomaterials and their surroundings are less understood. Here, we explore interactions between common serum proteins – serum albumin, fibrinogen, and immunoglobulin G – and a nanotextured gallium nitride surface. Atomic force microscopy with a carboxyl-terminated colloid tip is used to probe the 'activity' of proteins adsorbed to the surface, including both the accessibility of the terminal amine to the tip as well as potential for protein extension. By evaluating the frequency of tip-protein interactions, we can establish differences in protein behaviour on the basis of both surface roughness as well as morphology, providing an assessment of the role of surface texture in dictating protein-surface interactions. Unidirectional surface features – either the half-unit cell steppes of as-grown GaN or those produced by mechanical polishing – appear to promote protein accessibility, with a higher frequency of protein extension events taking place on these surfaces when compared with less ordered surface features. Development of a full understanding of the factors influencing surface-biomolecule interactions can pave the way for specific surface modification to tailor the bio-material interface, offering a new path for device optimization.

1 Introduction

Exploring the changes in properties and characteristics that take place when working with nanostructured vs. bulk materials dominates a significant portion of current scientific discussion across all areas of materials research. The phenomena that arise when working with these increasingly small length scales offer great promise and potential for streamlining device construction and optimizing the performance of materials in a wide range of applications. Of particular interest in the realm of biomaterials design and development is the comparatively newfound ability to produce well-defined structures and textures that approximate the size scale of biomolecules[1, 2]. In the nanoscale, complex biofluids present an extraordinarily complex colloidal system of ions, proteins, and other molecular and macromolecular structures. Successfully interfacing with this environment, as might be desired in constructing a biosensor for monitoring biomarker levels or a probe for communicating with neurons, will involve a careful consideration of these factors to optimize the biomolecule-surface interactions that dictate device function[3, 4].

The use of semiconductors for bio-interfacing presents one potential route for developing said biosensors or probes given their role in functional devices. Field effect transistor (FET) architectures have been extensively discussed for these applications[4], with various materials exhibiting more or less promising characteristics associated with not just electrical properties but biocompatibility[5] and potential for surface functionalization[6, 7]. Gallium nitride (GaN) has emerged as a promising candidate for these reasons – in addition to having a wide band gap (3.4 eV[8]), GaN has demonstrable biocompatibility[9-11] and chemical stability[12], and has been incorporated into a heterojunction FET that successfully demonstrated minimal drift in ionic solutions[13]. It thus becomes worthwhile to investigate methods of optimizing the performance of a GaN surface in interfacing with complex biofluids such that desired interactions are promoted or maintained. Chemical modification of GaN – via both covalent functionalization[10, 14] as well as application of recognition

peptides[14, 15] – has been demonstrated in the literature, as have secondary studies demonstrating improvements in viability and development of cells cultured on chemically modified surfaces[10, 14]. Cell culture experiments have also progressed on topographically modified GaN surfaces[16]; by borrowing techniques developed by the photonics community, a range of surface features – including unidirectional grooves produced by mechanical polishing and pores etched in a photochemical process[17, 18] - can be introduced to the GaN surface.

Some early reports investigating protein adsorption to surface nanotexture indicated that there was no noticeable change in protein behaviour in response to surface nanotextures[19, 20]; however, several recent publications have disputed these earlier claims[21, 22]. Advancements in both analytical techniques for nanoscale surface analysis – including refinement of atomic force microscopy (AFM) and other imaging methods – as well as introduction of novel schemes for monitoring surface behaviour – such as using quartz crystal microbalance (QCM) to detect changes in the amount of adsorbed protein between two surfaces[21] – have offered improvements to the experimental nanoscience 'toolbox.' AFM, specifically, has been used to both characterize surface topography and viscoelasticity at the nanoscale as well as probe biomolecular interactions in a site-specific manner[23-27]. By preparing cantilever tips with desired surface chemistries or biomolecular functionalization, the interaction forces between these molecules and a sample surface (e.g. a carboxyl-terminated self-assembled monolayer (SAM)[24]) can be recorded. This has provided insight into the strength of interaction between said carboxyl-terminated SAM and albumin molecules[24], alkanethiolate SAMs and CH_3, NH_2, OH, or COOH-terminated probe tips[23], and a range of other probe-surface combinations[26-28].

The following report follows a systematic experimental procedure, wherein we measure the interaction between a colloid-tipped AFM probe with a specific surface chemistry and a surface of interest. Rather than modifying the AFM tip with the molecule of interest, however, we expose the material surface – GaN, with a defined surface topography – to the protein and record the subsequent tip-surface adhesion. Through assessment of both the measured adhesion force as well as the frequency of protein-related adhesion and extension events, we document the effect of a nanoscale surface topography on the adsorption and subsequent behaviour of common serum proteins on a GaN surface. Selected proteins include albumin, fibrinogen, and immunoglobulin G (IgG); all were chosen due to both the extensive characterization data available[23, 24, 29] as well as their prevalence within blood serum.

2 Materials and Methods

GaN Sample Growth and Preparation

Unintentionally doped Ga-polar gallium nitride was grown on c-plane sapphire by metalorganic chemical vapour deposition, producing a smooth morphology[30]. One GaN film was grown on a high temperature AlN layer, which was in turn grown on a low temperature AlN nucleation layer, allowing control of material polarity on a sapphire substrate. The resulting GaN film features a dislocation density of 1 x 10^9 cm^{-2} and a surface morphology dominated by growth spirals that arise from screw dislocations that intersect the growing surface. The other GaN film was only grown on the low temperature AlN nucleation layer. In this case, the surface morphology was dominated by step flow growth influenced by the miscut of the sapphire substrate.

For subsequent processing and treatment, the as-grown GaN wafer was diced into 3 x 3 mm^2 sections (American Precision Dicing; San Jose, CA.) Polished GaN was produced using conventional mechanical polishing with a 6 μm diamond slurry. This included mounting samples on metal chucks and subsequent polishing on a rotating polishing wheel for 90 seconds while holding the sample orientation constant. 90 seconds was sufficient to introduce surface features in a consistent manner based on subsequent topographic characterization, and in holding the sample 10 cm from the center of wheel rotation without changing the orientation of the sample the resulting features were nominally parallel. The etch process for the porous samples was adapted from prior work[18]. In brief, surfaces are cleaned and sputtered with platinum islands prior to the etch process. Samples were placed in the etchant, a 1:2:1 solution of 38% H_2O_2, 49% HF, and methanol, and left for one hour under a 100 W UV lamp. Multiple rinses in methanol and deionized water were used to remove etch residue.

Prior to imaging of clean samples or exposure to protein, samples were solvent cleaned via sonication in serial acetone, ethanol, and deionized water. A 10 minute etch in piranha solution (3:1;sulfuric acid to hydrogen peroxide) was performed to remove surface organic contaminants, followed by a 10 minute etch in HCl to remove the surface hydroxyl termination introduced via etching in piranha. Samples were rinsed with deionized water and dried with N_2 immediately prior to imaging (clean samples) or exposure to protein solutions.

Protein Treatment

Cleaned samples were incubated in a refrigerator at 4° C overnight (~18 hours) in a 20 μL droplet of protein solution. Protein solutions (protein dissolved in stock PBS, pH 7.4, prepared as directed from tablets; Sigma, Cat. #P4417) were initially prepared in accordance with the standard reference levels of a human blood metabolic panel; however, for experiments involving fibrinogen and IgG, this yielded an excessive degree of protein-tip attachment for the retraction distance used in force curve acquisition. As such, these concentrations were reduced by an order of magnitude to enable acquisition of data. Albumin was prepared to a 50 mg/mL concentration; IgG to 1 mg/mL; and fibrinogen to 300 μg/mL. After overnight incubation, samples were rinsed by dipping in PBS to remove unaffiliated protein and drifted with N_2 to dry.

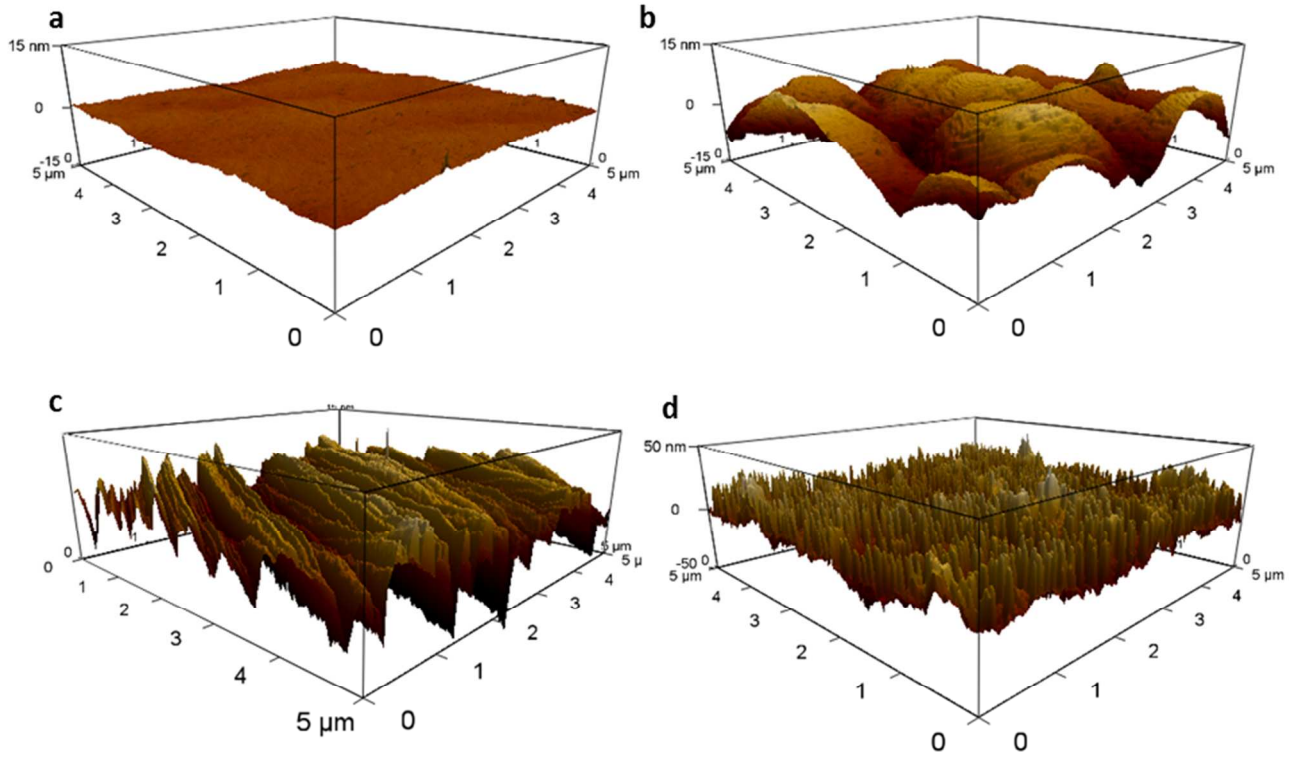

Figure 1 3D atomic force micrographs demonstrating the four surface morphologies. (a) As-grown lateral steppes, (b) as-grown spiral hillocks, (c) mechanically polished, and (d) photochemically etched GaN. Height range 30 nm in (a-c), 100 nm in (d).

Force Microscopy

Samples were mounted on AFM pucks using non-water soluble Crystalbond to avoid dissolution of adhesive during imaging and data collection in fluid. Experiments were conducted in a 60 µL volume of room-temperature PBS; temperature was monitored within the AFM chamber and remained at 25.8-26.2 ºC.

The Cypher atomic force microscope (Asylum Research, Santa Barbara, CA) was used for all AFM data acquisition. Root-mean-square (RMS) roughness for each surface topography was calculated based on the average of 5 x 5 µm height scans collected from each of three samples.

Tips used for contact mode imaging were standard SiN tips purchased from Asylum Research (TR800PSA.) For characterizing protein behaviour, carboxyl-terminated colloidal probe tips were ordered from Novascan. Gold-coated tips featured a 4.5 µm diameter polystyrene bead with a carboxyl-functionalized surface. A new tip was used for each surface-protein configuration, and tip resonance frequency and spring constant were monitored to verify the lack of protein buildup on the probe.

Data Analysis

AFM data were processed using Igor Pro software, with in-house algorithms for calculating adhesion force based on a force-distance curve. Subsequent data processing and visualization was conducted using MatLab and ImageJ. Statistical analysis was performed using SAS statistical analysis software. A one-sided ANOVA followed by Tukey-Kramer adjustment (α=0.05 significance level) was used to compare all surfaces and protein treatments as distinct configurations.

Table 1 Root-mean-square roughness values for the four GaN morphologies.

	Lateral	Hillock	Polished	Etched
R_{RMS}* (nm)	0.37 ± 0.02	3.4 ± 0.4	11.5 ± 3.2	9.3 ± 3.6

*Values presented as an average ± standard deviation (n=3-5 total topography maps from three different sample surfaces.)

3 Results and Discussion

Initial surface characterization included assessment of surface roughness; RMS roughness values and associated standard deviations are provided in **Table 1**. **Figure 1** provides complementary topography images demonstrating the clear differences in surface morphology – the hillock and etched surface both have more random/disordered features, while the lateral and polished feature unidirectional ridges. As a point of reference when considering scale and the potential for steric hindrance and size exclusion effects, **Figure 2** provides rendered representations and associated approximate dimensions for the three serum proteins used in this study. This provides a loose basis for size comparison between the surface features of the inorganic material and the proteins used in the

study, revealing that the semiconductor nanotextures are on the same scale as these biomolecules.

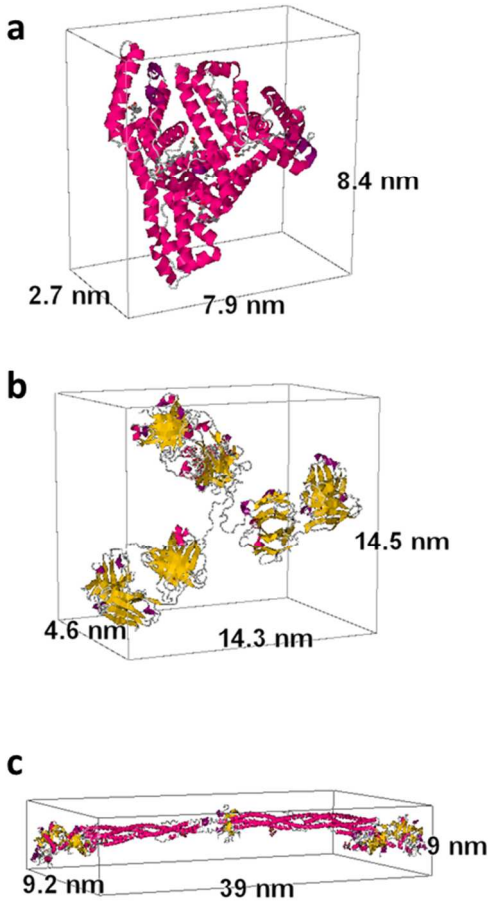

Figure 2 JMol renderings of (a) albumin (PDB 1E71{Bhattacharya, 2000}), (b) IgG (PDB 1IGT{Harris, 1997}), and (c) fibrinogen (PDB 1M1J{Yang, 2001}). Lengths correspond to the bounds of the box enclosing the molecule; dimensions are in agreement with the literature[23-25, 31]. Images from the RCSB PDB (www.rcsb.org); PDB ID given in parentheses.

Generating a meaningful comparison of adhesion data first requires separation of data into constituent 'types' of adhesion profiles[24], examples of which are given in **Figure 3**. Four characteristic adhesion profiles were observed – the first (Fig. 3a) is indicative of no tip-surface interaction. The approach and retraction of the tip overlap, with no evidence of surface interaction beyond the deflection caused by basic tip-surface contact. Surface adhesion alone is observed in Fig. 3b, indicative of short-range van der Waals and other non-covalent interactions. Protein extension events are seen in Fig. 3c-d, with 3c representative of an isolated extension and 3d indicating both surface adhesion and extension. "Protein extension" in truth describes a wider range of protein behaviours, including the stretching of folded domains, conformational changes, or just a gradual detachment of protein from the tip[23, 24]. In the case of the cleaned surface, some evidence of this more complicated adhesion profile is also observed; we attribute this interaction to the ions present in the phosphate-buffered saline used for imaging.

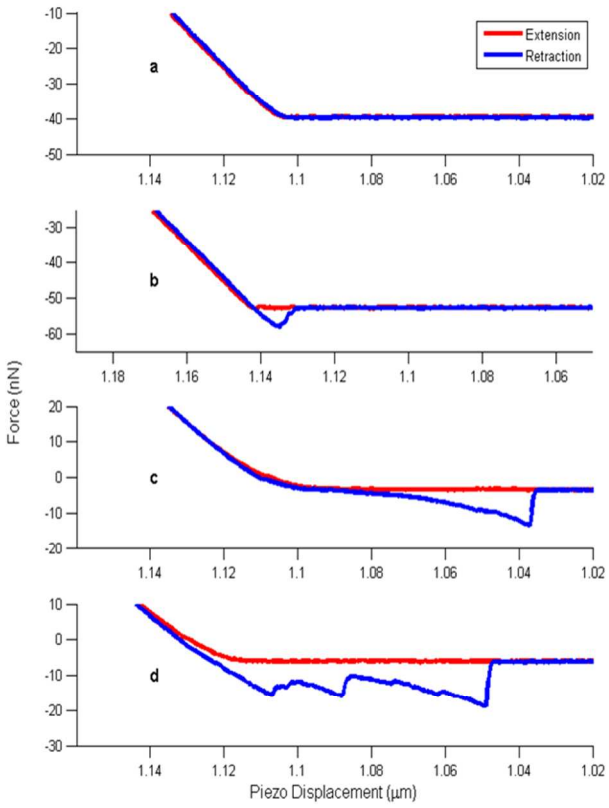

Figure 3 Representative approach/retract force curves for the four interaction classifications. (a) No adhesion – the approach and retract curves are indistinguishable. (b) Surface adhesion – a short-range attraction during the retract phase. (c) Protein extension – a longer-range interaction indicative of protein stretch following tip-surface contact without the characteristic peak associated with surface adhesion. (d) Surface adhesion and protein extension – an initial surface adhesion with subsequent, longer-range peaks indicative of extended protein-tip interactions.

While it is commonplace to assess the magnitude of adhesion in force characterization measurements of this nature, there is an extreme amount of variability in the data, even considering the division of data among the four archetypal behaviours shown in Fig. 3. An example of this is provided in the Supplemental Information; **Figure S1** provides the data and error bars representing standard deviation for the adhesion strength observed in surface adhesion-only curves (curve type shown in Fig. 3b.) Even with the removal of protein extension curves, which may involve various types of protein reorganization or unfolding, there is a high degree of variability in the data. As such, it becomes worthwhile to consider alternate routes of assessing the system under study to assert quantitatively distinct changes in behaviour across the nanotextured surfaces.

The results of one such alternate assessment are presented in **Figure 4**. Rather than assessing the rote adhesion force associated with a given category of adhesive event, the frequency of the different adhesion profiles is considered as a metric for establishing variations in protein-surface interaction. The percentage of the data wherein protein extension is

observed is plotted as a function of surface texture and protein modification. While ion-related extension is observed in the clean case, the introduction of albumin to the sample surface produces a statistically significant increase in the frequency of extension on both the lateral and polished GaN surfaces, and IgG or fibrinogen treatment produce this statistical distinction for all surfaces. Assessment of the data – particularly the changes observed on only the lateral and polished surfaces when comparing albumin-treated samples to clean – may now break down into a consideration of the surface features, molecule sizes, and molecular structure and function.

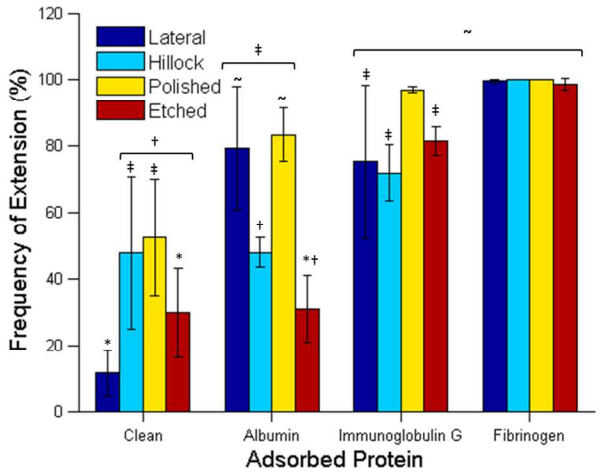

Figure 4 Percentage of the data featuring protein extension (curve archetypes seen in Fig. 3(c and d).) Matched symbols designate values that are statistically indistinguishable. There is a general increase in frequency of extension with the introduction of protein (as expected; in the clean case, these events are attributed to ionic interactions in the salt solution used for data collection.) Albumin and IgG feature the greatest distinction between distinct topographies, with the polished surface and as-grown lateral surface exhibiting a greater frequency of protein extension.

Albumin is the most abundant serum protein, playing a role in molecular transport within the body, and is typically the first protein to adsorb to a material surface following introduction to the body. This phenomenon and the subsequent displacement of albumin by other proteins with a greater affinity for the material surface has been characterized to the point of earning a specific title – the Vroman effect[32]. Figure 4 reveals a significant change in the frequency of protein extension events, but only on the surfaces with unidirectional features – the lateral and polished GaN. Hillock and etched surfaces are statistically indistinguishable from their clean counterparts. Compelling for the high specificity of binding to their complement molecules, immunoglobulins present one route of modifying a biosensor surface to bind and subsequently detect a specific antigen biomarker of interest[4]. Optimizing performance of such a device will rely in part on optimizing the availability of these antibody binding sites, a factor dependent on the conformation of the protein on the surface. Again, there is a statistically significant distinction between the surfaces – in this case, the polished surface demonstrates a greater frequency of protein extension than the other surfaces. The results emerging from adsorption of fibrinogen are not particularly surprising given the functional role of this protein in the body. Fibrinogen, when coupled with thrombin and platelet aggregates, plays a critical role in maintaining hemostasis through the formation of clots[25]. As such, the expectation (and subsequent observation) involves a degree of protein extension beyond that observed for albumin or IgG, with nearly all tip-surface interactions demonstrating protein extension (100% of the 1000+ force-distance curves taken on the hillock and polished surfaces indicated significant protein extension.) While the extent and frequency of protein extension prevents meaningful comparison between surfaces, the observation that fibrinogen is a particularly 'sticky' molecule meets expectations.

Delving into the behaviour observed for both albumin and, to a lesser extent, IgG can be related back to the nature of the topographies presented in Fig. 1. There is a marked increase in the frequency of protein extension on the polished surface and lateral surface – both of which feature approximately unidirectional topographies (a reduced-range image of the lateral surface to better emphasize this is provided in the supplemental information – **Figure S2.**) While determining the exact cause of this increase is difficult in the context of the current experiments, the observed trend suggests that unidirectional features at this scale promote either protein accessibility or adsorption. Increase in general quantity of adsorbed protein is a difficult assertion to make. The introduction of 'ordered' steric hindrance and size exclusion – factors that would promote protein adhesion to a ridge apex vs. the grooves on either side – does introduce some limitation to the GaN surface available for binding to the polished surface; however, a comparable effect of general hindrance could be expected for the etched surface, as well. Additionally, the scale of the feature sizes in the lateral surface is inadequate to extend such an effect to this surface. As such, we suggest that in this instance with these textures, the unidirectional features are able to promote protein accessibility for interaction with the COOH-terminated AFM probe. The nuance of conformational differences will require further characterization and evaluation to provide a clear picture of these changes; however, the statistically distinct increase in protein-related tip-surface interactions on the unidirectionally textured surfaces is indicative of a role of surface nanotexture in influencing the behaviour of adsorbed protein on a semiconductor material. One possible mechanism may again relate to 'ordered' vs. disordered steric hindrance associated with the surface features. By promoting adsorption of protein to the unidirectional features with an intermolecular spacing influenced by the distance between parallel ridges, a conformation that promotes interaction with the COOH-terminus of the probe becomes more thermodynamically favorable than alternate configurations. This shift in the population of 'accessible' protein may thus drive the change in interaction frequency, producing the statistically distinct increase in adhesion events on these unidirectional surface feautres.

4 Conclusions

The high degree of variability in full extent of adhesion renders rote comparison of protein extension events difficult; however, observing the frequency of specific tip-surface interactions offers a more conclusive observation of protein behaviour as a function of underlying surface texture. Distinct differences in adhesion characteristics emerge on the lateral and polished surface (both involving approximately unidirectional features) following any protein exposure; however, on the hillock and etched surfaces, there is no significant change when comparing the cleaned and albumin-treated surfaces. While there is no statistically significant difference in the frequency of protein extension across all surfaces following IgG or fibrinogen treatment, the presence of a distinct difference among surfaces following albumin exposure does indicate some variation in protein adsorption and subsequent behaviour depending on the nanoscale surface texture. As such, the results agree with what recent literature has started to suggest: that nanoscale surface textures can be used to modify protein and biomolecule behaviour on a material surface.

Acknowledgements

We thank ARO under W911NF-14-1-0664 for support of this work. I.B. would like to acknowledge the NDSEG Fellowship under and awarded by DoD, Air Force Office of Scientific Research, 32 CFR 168a.

Notes and references

[a] UNC/NCSU Joint Department of Biomedical Engineering, North Carolina State University. Engineering Building 3, 911 Partners Way, Raleigh, NC 27606.
[b] Department of Materials Science and Engineering, North Carolina State University. Engineering Building 1, 911 Partners Way, Raleigh, NC 27606.

Electronic Supplementary Information (ESI) available: Additional figures demonstrating adhesion force magnitude (Fig. S1) and lateral steppe surface topography (Fig. S2.) See DOI: 10.1039/b000000x/

1. A. E. Nel, L. Madler, D. Velegol, T. Xia, E. M. V. Hoek, P. Somasundaran, F. Klaessig, V. Castranova and M. Thompson, *Nature Materials*, 2009, **8**, 543-557.
2. N. Huebsch and D. J. Mooney, *Nature*, 2009, **462**, 426-432.
3. K. B. Cederquist and S. O. Kelley, *Current Opinion in Chemical Biology*, 2012, **16**, 415-421.
4. M. S. Makowski and A. Ivanisevic, *Small*, 2011, **7**, 1863-1875.
5. W. Hallstrom, T. Martensson, C. Prinz, P. Gustavsson, L. Montelius, L. Samuelson and M. Kanje, *Nano Letters*, 2007, **7**, 2960-2965.
6. R. J. Hamers, in *Annual Review of Analytical Chemistry*, Annual Reviews, Palo Alto, 2008, vol. 1, pp. 707-736.
7. M. Stutzmann, J. A. Garrido, M. Eickhoff and M. S. Brandt, *Physica Status Solidi a-Applications and Materials Science*, 2006, **203**, 3424-3437.
8. F. A. Ponce and D. P. Bour, *Nature*, 1997, **386**, 351-359.
9. C. R. Chen and T. H. Young, *Biomaterials*, 2008, **29**, 1573-1582.
10. S. A. Jewett, M. S. Makowski, B. Andrews, M. J. Manfra and A. Ivanisevic, *Acta Biomaterialia*, 2012, **8**, 728-733.
11. L. R. Bernstein, *Pharmacological Reviews*, 1998, **50**, 665-682.
12. C. M. Foster, R. Collazo, Z. Sitar and A. Ivanisevic, *Langmuir*, 2013, **29**, 216-220.
13. S. Gupta, M. Elias, X. Wen, J. Shapiro, L. Brillson, W. Lu and S. C. Lee, *Biosensors and Bioelectronics*, 2008, **24**, 505-511.
14. C. M. Foster, R. Collazo, Z. Sitar and A. Ivanisevic, *Langmuir*, 2013, **29**, 8377-8384.
15. E. Estephan, C. Larroque, F. J. G. Cuisinier, Z. Balint and C. Gergely, *Journal of Physical Chemistry B*, 2008, **112**, 8799-8805.
16. L. E. Bain, R. Collazo, S. H. Hsu, N. P. Latham, M. J. Manfra and A. Ivanisevic, *Acta Biomaterialia*, 2014, **10**, 2455-2462.
17. L. Santinacci and T. Djenizian, *Comptes Rendus Chimie*, 2008, **11**, 964-983.
18. D. J. Diaz, T. L. Williamson, I. Adesida, P. W. Bohn and R. J. Molnar, *Journal of Vacuum Science & Technology B*, 2002, **20**, 2375-2383.
19. M. Han, A. Sethuraman, R. S. Kane and G. Belfort, *Langmuir*, 2003, **19**, 9868-9872.
20. M. S. Lord, M. Foss and F. Besenbacher, *Nano Today*, 2010, **5**, 66-78.
21. N. Giamblanco, E. Martines and G. Marletta, *Langmuir*, 2013, **29**, 8335-8342.
22. L. Gailite, P. E. Scopelliti, V. K. Sharma, M. Indrieri, A. Podesta, G. Tedeschi and P. Milani, *Langmuir*, 2014, **30**, 5973-5981.
23. S. Kidoaki and T. Matsuda, *Langmuir*, 1999, **15**, 7639-7646.
24. M. A. Rixman, D. Dean, C. E. Macias and C. Ortiz, *Langmuir*, 2003, **19**, 6202-6218.
25. T. S. Tsapikouni and Y. F. Missirlis, *Colloids and Surfaces B-Biointerfaces*, 2007, **57**, 89-96.
26. J. J. Valle-Delgado, J. A. Molina-Bolivar, F. Galisteo-Gonzalez, M. J. Galvez-Ruiz, A. Feiler and M. W. Rutland, *Langmuir*, 2006, **22**, 5108-5114.
27. M. S. Wang, L. B. Palmer, J. D. Schwartz and A. Razatos, *Langmuir*, 2004, **20**, 7753-7759.
28. P. Roach, D. Farrar and C. C. Perry, *Journal of the American Chemical Society*, 2006, **128**, 3939-3945.
29. M. A. Rixman, D. Dean and C. Ortiz, *Langmuir*, 2003, **19**, 9357-9372.
30. S. Mita, R. Collazo, A. Rice, R. F. Dalmau and Z. Sitar, *Journal of Applied Physics*, 2008, **104**, -.
31. Y. H. Tan, M. Liu, B. Nolting, J. G. Go, J. Gervay-Hague and G. Y. Liu, *Acs Nano*, 2008, **2**, 2374-2384.
32. L. Vroman and A. L. Adams, *Acs Symposium Series*, 1987, **343**, 154-164.

